MIT Open Access Articles

Pressure-induced phase transformations during femtosecond-laser doping of silicon

Massachusetts Institute of Technology

Pressure-induced phase transformations during femtosecond-laser doping of silicon

Matthew J. Smith, Yu-Ting Lin, Meng-Ju Sher, Mark T. Winkler, Eric Mazur et al.

Additional information on J. Appl. Phys.

Pressure-induced phase transformations during femtosecond-laser doping of silicon

Matthew J. Smith,[1] Yu-Ting Lin,[2] Meng-Ju Sher,[3] Mark T. Winkler,[3] Eric Mazur,[2,3] and Silvija Gradečak[1,a)]

[1]*Department of Materials Science and Engineering, Massachusetts Institute of Technology, Cambridge, Massachusetts 02139, USA*
[2]*School of Engineering and Applied Sciences, Harvard University, Cambridge, Massachusetts 02138, USA*
[3]*Department of Physics, Harvard University, Cambridge, Massachusetts 02138, USA*

Silicon hyperdoped with chalcogens via femtosecond-laser irradiation exhibits unique near-unity sub-bandgap absorptance extending into the infrared region. The intense light-matter interactions that occur during femtosecond-laser doping produce pressure waves sufficient to induce phase transformations in silicon, resulting in the formation of metastable polymorphic phases, but their exact formation mechanism and influence on the doping process are still unknown. We report direct observations of these phases, describe their formation and distribution, and consider their potential impact on sub-bandgap absorptance. Specifically, the transformation from diamond cubic Si-I to pressure-induced polymorphic crystal structures (amorphous Si, Si-XII, and Si-III) during femtosecond-laser irradiation was investigated using scanning electron microscopy, Raman spectroscopy, and transmission electron microscopy. Amorphous Si, Si-XII, and Si-III were found to form in femtosecond-laser doped silicon regardless of the presence of a gaseous or thin-film dopant precursor. The rate of pressure loading and unloading induced by femtosecond-laser irradiation kinetically limits the formation of pressure-induced phases, producing regions of amorphous Si 20 to 200 nm in size and nanocrystals of Si-XII and Si-III. The surface texturing that occurs during femtosecond-laser irradiation produces inhomogeneous pressure distributions across the surface and causes delayed development of high-pressure silicon polymorphs over many laser pulses. Finally, we find that the polymorph phases disappear during annealing more rapidly than the sub-bandgap absorptance decreases, enabling us to decouple these two processes through post-treatment annealing. © *2011 American Institute of Physics*. [doi:10.1063/1.3633528]

I. INTRODUCTION

Silicon-based optoelectronic devices that operate at photon energies that are less than the silicon bandgap (1.1 eV) have been fabricated using femtosecond (fs) laser doping.[1] This process drives concentrations of chalcogen atoms in silicon to levels several orders of magnitude beyond their equilibrium solubility limit and produces hyper-doped silicon that exhibits near-unity absorption in the infrared (IR) region, at wavelengths to which crystalline silicon is transparent.[2–4] Such properties are not achievable through equilibrium doping techniques, and the ability to tune the band structure of silicon with fs-laser doping makes this process of great interest for IR-photodetectors[1] and photovoltaics.[5]

Femtosecond-laser irradiation induces a complex series of processes in a material before the energy is completely dissipated,[6] including melting, dopant incorporation, ablation, self-organized structure formation, and pressure or resolidification-velocity driven phase transformations. The surface morphology of silicon evolves over many laser pulses through melting and ablation processes. Initially, ripples with a periodicity related to the wavelength of the laser light form on the surface.[7] These ripples, known as laser-induced periodic surface structures, transform into micron-scale spikes with continued laser irradiation.[8] The formation and growth of surface spikes is driven by material ablation and has been studied in silicon for surface texturing for photovoltaics[9] and surface enhanced Raman spectroscopy,[10] and it is also observed during fs-laser doping under certain conditions.[1,11]

Material ablation during the fs-laser irradiation of silicon generates recoil pressure waves that rise sharply over a few picoseconds and decay over tens of picoseconds.[12,13] Such ultra-fast pressure cycles can drive pressure-induced phase transformations in silicon,[14–16] but the mechanisms and kinetics of pressure-induced phase transformations during fs-laser irradiation have not been thoroughly investigated.

The current understanding of pressure-induced phase transformations in silicon was developed through high pressure studies using diamond anvil cells[17] and nanoindentation.[18] From these studies, it is known that silicon transforms from its diamond cubic phase (Si-I) to a β-Sn phase (Si-II) at pressures above $\sim$12 GPa and that this transformation is irreversible, i.e., Si-II cannot transform back to Si-I during pressure unloading.[19,20] Upon sufficiently slow pressure release, silicon with an R8 structure (Si-XII) nucleates from Si-II and then reversibly transforms to a BC8 structure (Si-III) at

---
a)Author to whom correspondence should be addressed. Electronic mail: gradecak@mit.edu.

around 2 GPa.[21] Nanoindentation studies have found that the formation of Si-XII/III from Si-II is nucleation limited; alternatively, there is no activation barrier to the formation of amorphous silicon (a-Si) from Si-II. In other words, the nucleation of Si-XII/III can be suppressed by sufficiently fast unloading rates, forcing Si-II to transform completely into a-Si.[22] The silicon polymorphs that form during high-pressure cycles are metastable: Si-XII, Si-III, and a-Si transform back to polycrystalline Si-I with annealing through intermediate phases, although the exact pathway depends strongly on the surrounding matrix, residual stresses in the material,[23] the loading and unloading rates, the indenter shape,[22] the phase of the initial surface (a-Si versus c-Si),[24] and the ambient temperature.[25]

These nanoindentation studies provide some insights into the pressure-induced transformations in silicon, but the pressure generation mechanisms and pressure-induced phase transformations during the fs-laser irradiation of silicon around the ablation threshold are far from being elucidated. In addition to developing our fundamental understanding of fs-laser-material interactions, understanding pressure-induced phase transformations during fs-laser doping for optoelectronic applications is significant because a-Si, Si-III, and Si-XII have different material properties than Si-I and could affect optoelectronic device performance. For example, Si-XII has an indirect bandgap of 230 meV,[26] Si-III is a p-type semimetal,[27] and unpassivated a-Si presents a high density of recombination sites.

In this work, we investigate the relationship between laser-doping process parameters and the resulting high-pressure phase transformations. We investigate the spatial distribution of the silicon polymorphs in fs-laser doped silicon and show that they form preferentially in the center of the surface spikes. The mechanism by which high-pressure phases form only after multiple laser pulses is studied by monitoring the formation of Si polymorphs in fs-laser doped silicon with an increasing number of laser pulses. Finally, we investigate the thermal stability of silicon polymorphs formed during fs-laser irradiation and compare the kinetics of their relaxation with annealing to the evolution of the optical properties of fs-laser doped silicon with annealing. In addition to furthering the fundamental knowledge of fs-laser-material interactions, an understanding of pressure-induced phase transformations during fs-laser doping will enable the improved synthesis of hyper-doped materials for optoelectronic applications.

II. EXPERIMENT

Silicon (100) wafers (n-type, 3000 to 6000 Ω cm) were irradiated with Ti:sapphire fs-laser pulses (800 nm wavelength, 80 fs pulse duration, 700 μm spot size) at a fluence of 4 kJ/m^2. We compare silicon irradiated in N$_2$ (N$_2$:Si), for which we do not expect dopant incorporation or compositional changes during irradiation, to silicon fs-laser doped with S and Se. Silicon was fs-laser doped with sulfur (SF$_6$:Si) by irradiating the wafer in 500 Torr SF$_6$ gas. Silicon was fs-laser doped with selenium (Se:Si) by depositing a 70 nm Se thin film onto the wafer prior to fs-laser irradiation in

500 Torr N$_2$. Large areas of each sample were prepared by translating the silicon wafer during pulsed-laser irradiation such that, unless otherwise noted, every point on the sample surface received an equivalent 88 laser pulses. Additional details of the fs-laser doping process can be found elsewhere.[11] In order to investigate the formation mechanism of silicon polymorphs over many laser pulses, Se:Si was prepared with an increasing number of laser pulses (10, 25, 42, and 88). Finally, in order to investigate the thermal stability of the silicon polymorphs, Se:Si prepared with a fluence of 4 kJ/m^2 and 88 pulses was annealed in a N$_2$ atmosphere for 30 min at different temperatures (325 °C, 450 °C, 575 °C, and 700 °C).

Raman spectroscopy was used to detect the presence of high-pressure silicon phases, compare their relative volumes, and investigate the residual stress present in these phases. The formation of silicon polymorphs was studied using a Raman spectrometer with a 10 mW 632.8 nm HeNe laser, recorded through a 20× objective (0.4 NA) with a spot size of 10 μm, and projected onto a CCD using a 1200 g/mm diffraction grating. In order to quantify the Raman investigations, spectra were collected from 20 different locations on each sample. The averaged peak positions and intensities (defined as the area under each background-subtracted peak), as well as their respective standard deviations, were determined. The infrared absorptance was measured with an ultraviolet-visible-near infrared (UV-VIS-NIR) spectrophotometer. The infrared transmittance (T) and reflectance (R) were measured with an UV-VIS-NIR spectrophotometer equipped with an integrating sphere and used to calculate the absorptance ($A = 1 - R - T$).

The sample morphology was investigated using an FEI Helios 600 scanning electron microscope (SEM) operated at a 5 kV accelerating voltage. Cross-sectional transmission electron microscopy (TEM) samples were prepared using a tripod polisher followed by a brief Ar$^+$-ion mill at 5 kV. Bright-field (BF)-TEM micrographs and selected area diffraction patterns were collected with a JEOL 2011 TEM operated at 200 kV. Selected area diffraction (SAD) patterns for the crystalline silicon crystal structures were calculated using the JEMS software package. Dark-field scanning TEM (DF-STEM), convergent beam electron diffraction (CBED), and electron energy loss spectroscopy (EELS) were carried out on a JEOL 2010 F TEM operated at 200 kV, with a Gatan image filtering (GIF) system with an energy resolution of 1.2 eV. To remove noise without affecting the overall shape, the reported EELS spectra were processed using an 8-point Savitzky-Golay smoothing filter.

III. RESULTS

A. Silicon polymorph formation during fs-laser doping

First, the relationship between silicon polymorph formation and the introduction of dopants during fs-laser irradiation was investigated using Raman spectroscopy; peak positions and relative peak intensities in the Raman spectra were used to understand the extent of the phase transformations and their resulting stress states. All three samples investigated—N$_2$:Si (reference), SF$_6$:Si, and Se:Si—develop

micron-scale spikes on the surface after 88 fs-laser pulses (Fig. 1(a)) and exhibit peaks in the Raman spectra indicative of Si-XII (354 cm^{-1}, 395 cm^{-1}), Si-III (387 cm^{-1}, 443 cm^{-1}), and a-Si (broad peaks at 150 cm^{-1}, 300 cm^{-1}, and 470 cm^{-1}) (Fig. 1(b)).[28] The intensities of the silicon polymorph Raman modes are at least an order of magnitude lower than the Si-I peak at 519 cm^{-1}, suggesting that a relatively small volume of silicon polymorphs is generated compared to Si-I.

We estimated the residual strain in the high-pressure crystalline polymorphs by measuring the position of the Si-III peak around 443 cm^{-1} and the Si-XII peak around 354 cm^{-1} (these peaks were selected because they are the most clearly pronounced Raman modes of their respective phases (Fig. 1(b))). Though small variations (1 to 2 cm^{-1}) exist among the 20 spectra recorded at different positions on each

sample, the Si-XII and Si-III peaks are consistently shifted to significantly higher wavenumbers (4 to 10 cm^{-1}) than the typical values reported in nanoindentation studies,[29] suggesting that they exist under compressive stress. The appearance of 2 characteristic peaks for both Si-XII (354 cm^{-1}, 395 cm^{-1}) and Si-III (387 cm^{-1}, 443 cm^{-1}) confirms that these peaks originate from the crystalline polymorphs despite their sizable shift. Finally, the volume ratio of the Si-XII and Si-III generated was estimated from the Raman peak intensities at 443 and 354 cm^{-1} (Fig. 1(c)). N$_2$:Si, SF$_6$:Si, and Se:Si have a Si-XII/Si-III ratio greater than unity, suggesting that the majority of the total crystalline polymorph volume is Si-XII.[29]

B. Spatial distribution of silicon polymorphs

Next, we investigated the spatial distribution of silicon polymorphs using TEM to gain insight into the polymorph formation process and the pressure profiles induced during fs-laser irradiation. The general structure of the N$_2$:Si and SF$_6$:Si surface spikes (Figs. 2(a) and 2(b), respectively) is consistent with our previous investigations.[30] Irradiation in N$_2$ (N$_2$:Si) produces a 300 to 500 nm thick surface layer (Fig. 2(a)), formed through laser-induced melting and resolidification (melt depth). A disordered surface layer with 1%
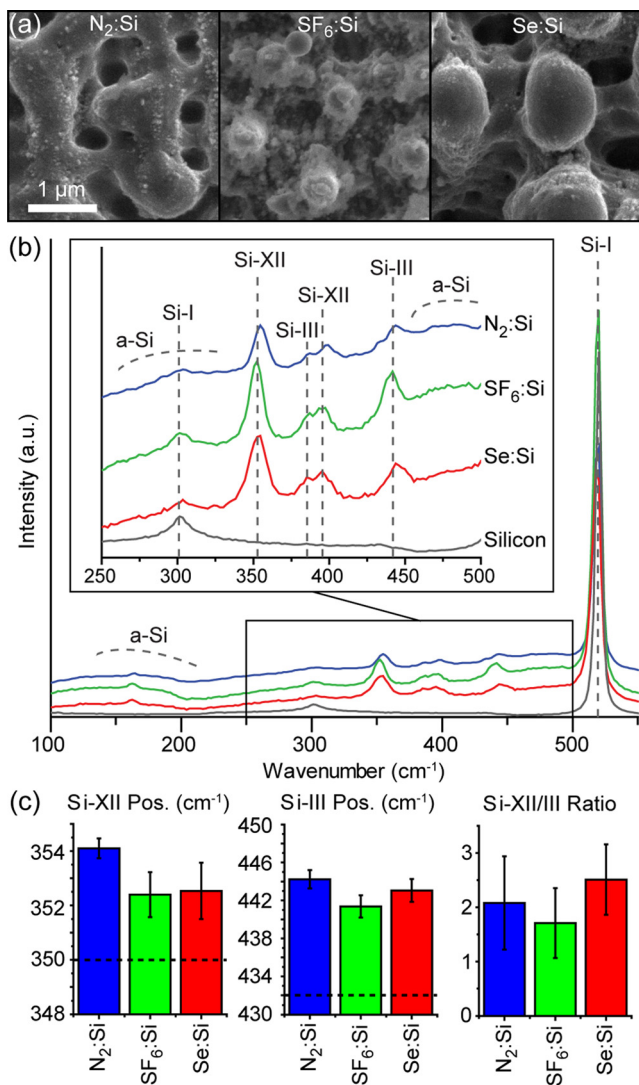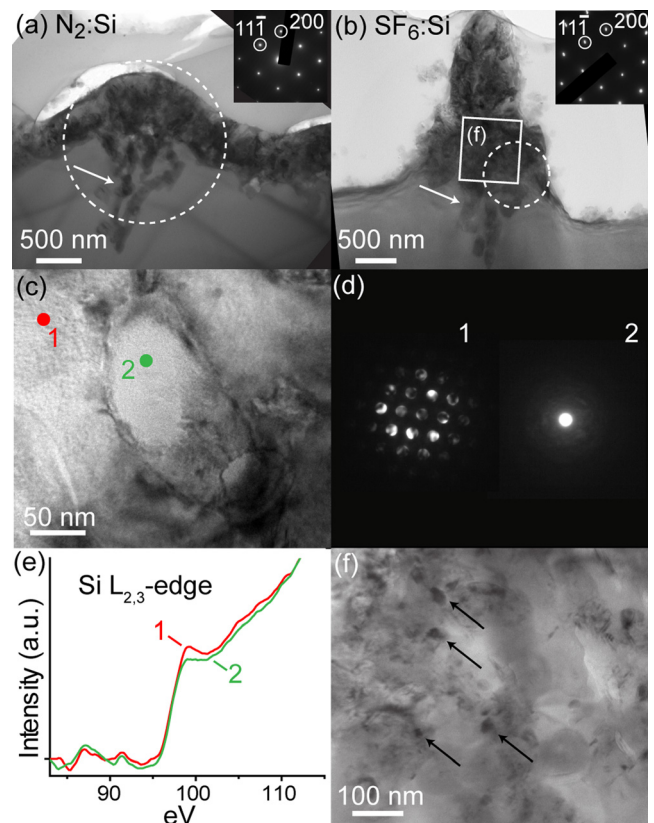

FIG. 1. (Color online) (a) SEM micrographs showing the surface morphology of fs-laser irradiated Si. The laser scan direction and polarization were in the horizontal direction. (b) Stokes Raman spectra of SF$_6$:Si, Se:Si, and N$_2$:Si, offset to show individual spectra. The rescaled inset highlights the Raman modes corresponding to a-Si, Si-III, and Si-XII. The color designation is the same in both plots. (c) The position of the Si-XII and Si-III modes and their relative intensities. Dashed lines indicate the positions of the Si-XII (350 cm^{-1}) and Si-III (432 cm^{-1}) Raman modes reported in nanoindentation studies (Ref. 29).

FIG. 2. (Color online) Cross-sectional BF-TEM images of N$_2$:Si (a) and SF$_6$:Si (b). SAD patterns from the regions highlighted by the dashed circles (inset) correspond to the Si-I [101] zone axis. White arrows indicate contrast in the core of the peaks arising from 20 nm to 200 nm areas of transformed material shown to be a-Si. (c) BF-TEM image of an isolated region of a-Si from the core of a SF$_6$:Si spike. Numbered spots correspond to points probed using CBED (d) and EELS (e). (f) BF-TEM image of the region in (b) that shows nanocrystals (black arrows) inside the a-Si.

atomic concentrations of sulfur forms during irradiation in SF_6; it is thinner than the melt depth in N_2:Si because SF_6 chemically etches silicon during laser irradiation. Although the SAD patterns show that the spikes are mostly single-crystalline c-Si (Figs. 2(a) and 2(b), inset), both samples exhibit strong contrast in the center of the spike, a finding that we assign to local strain variations in the c-Si matrix.

We identify the strain contrast as being caused by isolated regions of a-Si (20 to 200 nm) within the surrounding c-Si matrix, as discussed below. A single region from the center of a SF_6:Si spike is shown in Fig. 2(c), and the CBED patterns (Fig. 2(d)) confirm that the volume of material is amorphous and the surrounding matrix is crystalline. The EELS spectra reveal no chemical difference between the volume of amorphous material and the c-Si matrix. However, the fine structure of the Si-L_{23} edge (99 eV; Fig. 2(d)) measured in the amorphous region exhibits a shoulder at 102 eV, in contrast to the dip exhibited in the spectra from the c-Si matrix. This fine structure is characteristic of a-Si, resulting from the reduction of the density of states around the conduction-band minimum in a-Si.[31,32] We note that a-Si can form through melting and ultra-fast resolidification following fs-laser irradiation under certain conditions,[15,33] but we do not observe such a-Si layers on the surface, and the a-Si particles are found in regions below the melt depth.

Within the a-Si regions we observe nanocrystals 1 to 10 nm in size (Fig. 2(f)). The small size of the nanocrystals makes them undetectable by SAD, and their structure is difficult to confirm, but we expect Si-XII and Si-III to be present within the a-Si regions because both a-Si and the crystalline polymorphs are products of the initial transformation to Si-II, and they will therefore be present in the same regions. In addition, the formation of a-Si can promote the nucleation of crystalline polymorphs during subsequent laser pulses, as the activation barrier of nucleating Si-XII from Si-II is greatly reduced at the Si-II–a-Si interface.[25] For these reasons, it is likely that the nanocrystals in the a-Si regions are nucleated Si-XII and/or Si-III. We also note that if larger volumes of Si-XII/III were present in the bulk but relaxed to Si-I during sample preparation, they would form nanocrystalline Si-I, which was not observed.

In contrast to the single-crystalline structure of N_2:Si and SF_6:Si surface spikes, the Se:Si spikes are composed of Se-rich polycrystalline silicon (pc-Si) (Fig. 3(a)), arising from the use of a thin-film dopant precursor, as we reported previously.[30] We were not able to identify a-Si in the spike due to the strong diffraction contrast of this polycrystalline region, but a-Si regions can be observed in the single-crystalline base of the spike. In addition, a single crystal of Si-III on the [101] zone axis was identified within the polycrystalline region using SAD (Fig. 3(b)); this diffraction pattern is most easily identifiable by (101) spots corresponding to a spacing of 4.70 Å.[34]

C. Silicon polymorph formation and evolution over many laser pulses

To further investigate the high-pressure phase transformations, we monitored the formation of silicon polymorphs
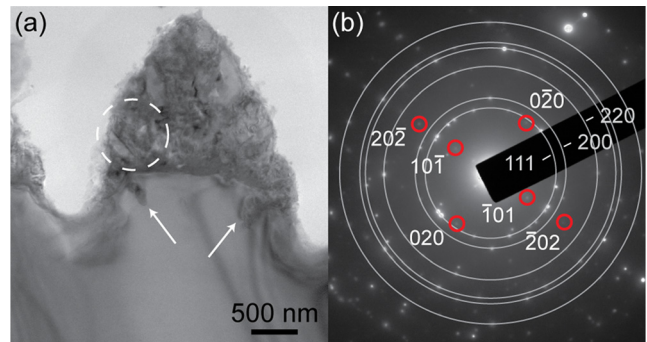

FIG. 3. (Color online) (a) BF-TEM image of Se:Si peak showing a polycrystalline region and small volumes of a-Si (arrows). (b) SAD pattern from the region corresponding to the dashed circle in (a). Spots corresponding to the Si-III [101] zone axis can be identified within the Si-I polycrystalline pattern (rings), and lower order spots are identified by circles.

in Se:Si with an increasing number of fs-laser pulses using Raman spectroscopy. SEM images of the surface morphology evolution as a function of the number of laser pulses (Fig. 4(a)) show the evolution of spikes from ripples over multiple laser pulses. The corresponding Raman spectra (Fig. 4(b)) reveal that the broad a-Si peak and the Si-XII/III polymorph peaks appear after 25 laser pulses, which coincides with the transition from the initial ripples on the surface to micron scale spikes. No significant trends in the position of the Si-XII and Si-III modes (Fig. 4(c)) with an increasing number of laser pulses were observed, but the Si-XII/Si-III ratio (Fig. 4(c)) increases between 25 and 88 laser pulses, indicating that Si-XII is preferentially generated over Si-III in this stage of laser irradiation. With higher numbers of laser pulses, the surface becomes difficult to characterize using Raman spectroscopy due to the rapidly increasing surface roughness.

D. Annealing of high-pressure phases formed by fs-laser irradiation

Silicon that is fs-laser doped with chalcogens exhibits strong sub-bandgap absorptance that decreases drastically with annealing.[11] Because pressure-induced silicon polymorphs are also metastable and transform back to Si-I with annealing, we compare the relative rates of relaxation of silicon polymorphs and optically active chalcogen species in order to gain insight into the relationship between these two processes. Selenium fs-laser doped silicon (Se:Si) was annealed for 30 min in nitrogen at 325 °C, 450 °C, 575 °C, and 700 °C, and the average absorptance was measured for each and compared to N_2:Si and untreated Si (Fig. 5(a)). We observed a characteristic decrease in the sub-bandgap absorptance of Se:Si with annealing, from 90% prior to annealing to 44% after the 700 °C anneal. The monotonically decreasing absorptance in N_2:Si is likely due to defect states induced by irradiation.[11]

The evolution of the silicon polymorphs with annealing was monitored using Raman spectroscopy (Fig. 5(b)). The Si-XII and Si-III modes are still visible after annealing at 325 °C, but they cannot be resolved after the 450 °C anneal. The 325 °C anneal did not significantly change the position
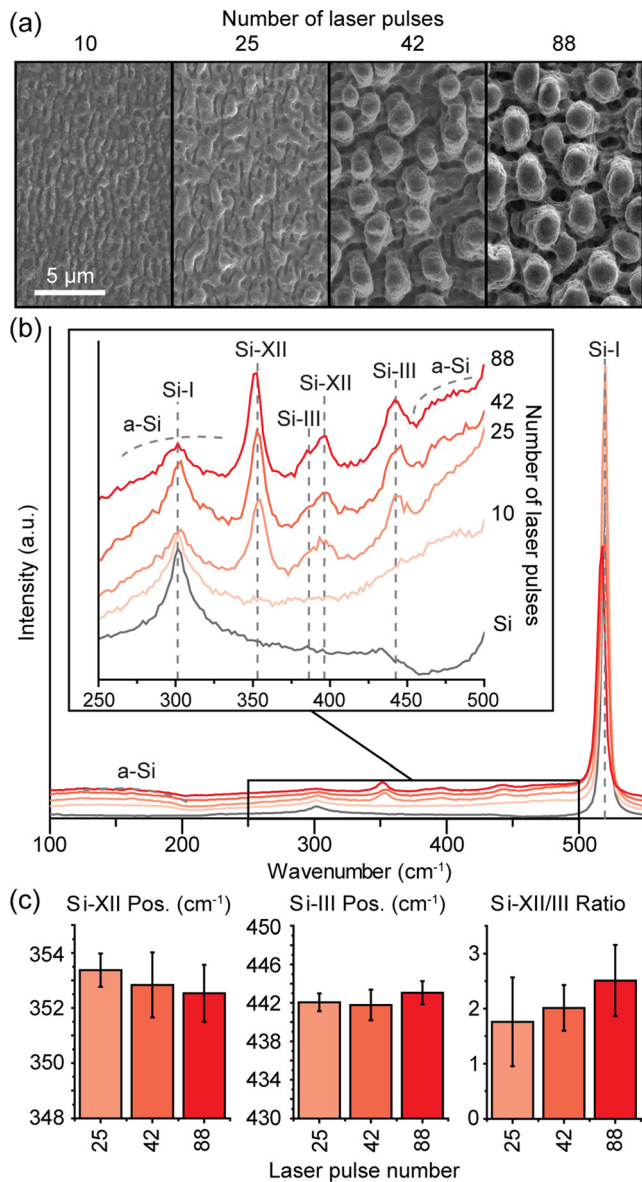
FIG. 4. (Color online) (a) SEM micrographs of the Se:Si surface morphology evolution with increasing laser pulse number. The laser scan direction and polarization were in the horizontal direction. (b) Stokes Raman spectra of Se:Si irradiated with an increasing number of laser pulses, offset to show the individual spectra. The inset is rescaled to highlight the Raman modes corresponding to a-Si, Si-III, and Si-XII. The color designation is the same in both plots. (c) Bar graphs showing the position of the Si-XII and Si-III modes and their relative intensities after 25, 42, and 88 laser pulses.
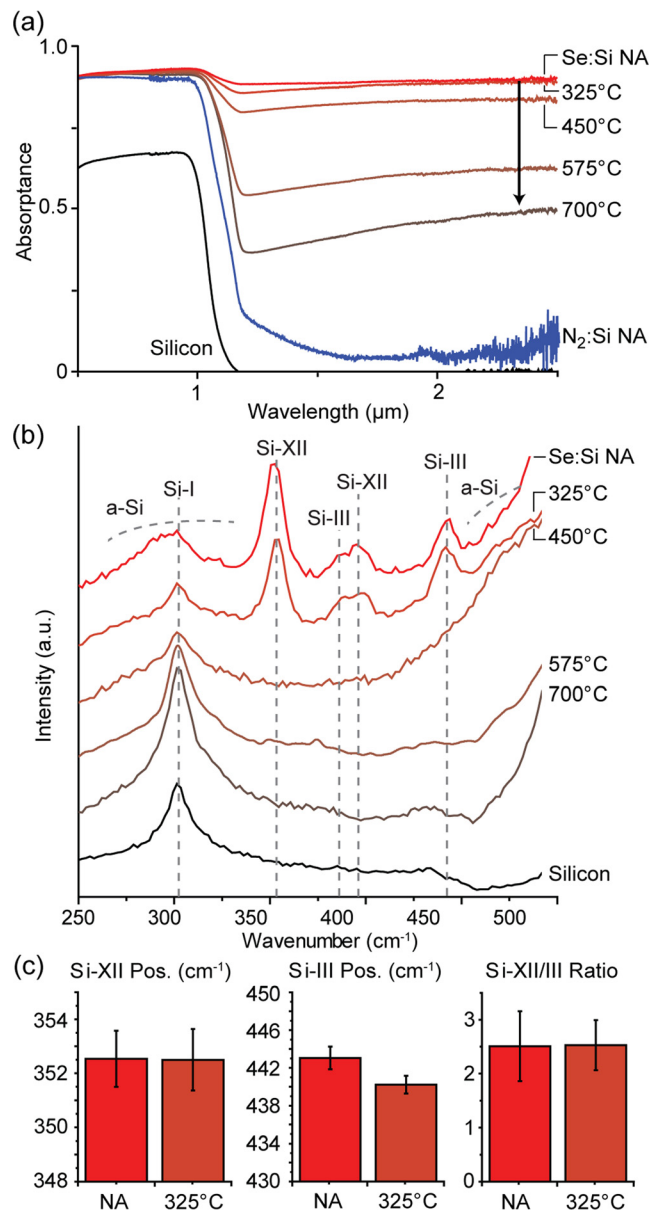

FIG. 5. (Color online) (a) Absorptance spectra of Se:Si after a 30 min anneal at the indicated temperatures. Included for reference are spectra from non-annealed (NA) Se:Si and N_2:Si, taken from Ref. 29, and from a silicon wafer. (b) Stokes Raman spectra of the same samples (250 to 500 cm^{-1}). The spectra are offset to highlight the a-Si, Si-III, and Si-XII peaks and their evolution with annealing. NA Se:Si is included for reference. (c) Bar graphs showing the position of the Si-XII and Si-III modes and their relative intensities with annealing.

of the Si-XII mode or the Si-XII/Si-III intensity ratio, as expected based on previous work.[35] The Si-III mode, however, is shifted to lower wavenumbers (Fig. 5(c)), which suggests a relaxation of the initial compressive stress with annealing. Finally, the broad a-Si peak at 470 cm^{-1} is still visible after the 575 °C anneal, but it disappears after the 700 °C anneal.

IV. DISCUSSION

A. Pressure-induced phase transformations during fs-laser doping

The variation of the Raman spectra (Fig. 1(c)) of silicon that had been fs-laser doped using different dopant precur-

sors was not significant, suggesting that the formation of silicon polymorphs is not directly coupled to the doping process, dopant type, or precursor phase. The Raman and TEM results reported in this paper, including the extent of the phase transformations, Raman peak intensities, and peak positions, can be instead attributed to the ultra-fast pressure loading and unloading that fs-laser irradiation induces. Our TEM investigations show that the transformation to a-Si is limited to 20 to 200 nm particles that form in close proximity to each other and in the center of the surface spikes. This volume reflects the material transformed to Si-II upon pressure loading, as Si-II cannot transform back to Si-I upon pressure release. We propose that the transformation to Si-II

is kinetically limited by the picosecond-scale duration of the pressure loading, and that the volume of a-Si reflects the extent of nucleation and growth of Si-II that occurred before pressure release. During nanoindentation investigations, slow, incremental loading conditions result in silicon polymorph formation over the entire volume subject to sufficient pressures for the Si-I→Si-II transformation.[24] In this scenario, the transformation does not suffer from kinetic limitations, and micron-scale volumes of a-Si and Si-XII/III are produced. In contrast, the small and kinetically limited volumes of Si-II generated in fs-laser irradiated Si are an important aspect of the phase transformation process, as the total volume of material transformed to Si-II will influence the subsequent phase transformation pathways. For example, the nucleation of Si-XII from Si-II is less probable in small volumes of Si-II due to the reduced number of available nucleation sites.[22]

It has been shown in nanoindentation studies that the probability of Si-XII and Si-III nucleation is suppressed by fast unloading conditions, which instead favor the formation of a-Si from Si-II,[29] and this is consistent with our observations. Only a limited amount of crystalline high-pressure phases was observed in BF-TEM images that show 1 nm to 10 nm nanocrystals within the a-Si volumes (Fig. 2(f)), which are most likely Si-XII and Si-III. The ultra-fast unloading conditions might also limit the subsequent Si-XII→Si-III transformation, as suggested by the preferred generation of Si-XII over Si-III during fs-laser irradiation (Fig. 1(c)).

The observed Raman peak shifts quantified in Fig. 1(b) can be qualitatively translated into residual stresses based on empirical studies of the Si-XII and Si-III peak positions with pressure; a shift of the Si-XII peak from 350 cm^{-1} to 354 cm^{-1} and of the Si-III Peak from 432 cm^{-1} to 443 cm^{-1} indicates that both crystalline silicon polymorphs exist under roughly 3 GPa of compressive stress.[36] Si-XII and Si-III are denser phases than Si-I, and it might be expected that they would form under tensile stress due to the encapsulating Si-I matrix; still, our results show that they exist in compressive stress. We speculate that the ultra-fast pressure release quenches Si-XII and Si-III phases in a high-pressure state such that they cannot relax to their equilibrium metastable structures.

B. Polymorph spatial distribution and evolution with shot number: An incubation effect

The BF-TEM investigations reveal that high-pressure silicon phases form preferably in the core of the spikes, suggesting that the pressure-induced phase transformations are related to the evolution of the surface morphology over multiple laser pulses. Transformed regions of material have been observed previously in the cores of peaks formed by the fs-laser irradiation of silicon,[37,38] but neither their composition nor their mechanism of formation has been explained. In addition, we see that the initial laser pulses do not generate sufficient pressures at this fluence (4 kJ/m^2) to drive phase transformation (Fig. 4(b)), but identical laser pulses during later-stage irradiation do. The spatial distribution and

delayed formation of the silicon polymorphs can be explained by the evolving surface morphology and the related ablation processes, as discussed below.

During femtosecond laser irradiation, recoil pressure waves form in reaction to the ablation of material from the surface.[16] The pressure generated is proportional to the amount of material ablated away and thus increases with laser fluence. As the initial laser induced periodic ripple structures grow into larger structures, light is preferentially reflected from the sides of the inclined surfaces and is focused into the valleys between spikes.[8] This increases the local laser fluence in the valley, which in turn increases the rate of ablation, and thus the magnitude of the pressure waves generated. The preferential ablation of material from the valleys creates the appearance that the surface spikes are growing with increasing shot number (Fig. 4(b)), and this creates a positive feedback loop. Whereas the average laser fluence remains constant, the evolving surface morphology creates localized regions of amplified fluence and subsequent recoil pressure waves, which eventually reach the critical values necessary to induce high-pressure phase transformations. Through this combination of processes, relatively low-fluence fs-laser irradiation can achieve very high pressures in localized areas on the surface. The presence of silicon polymorphs in the core of the spikes (Figs. 2(a) and 2(b)) also reveals that these regions achieved pressures higher than are experienced in the valleys. It is possible that the collision of pressure waves from multiple valleys is necessary in order to achieve sufficiently high pressures to drive phase transformations.

Our Raman investigations show that the phase transformations evolve over many laser pulses, providing strong evidence that the nature of the pressure cycles changes as well. The increase of the Si-XII/Si-III peak intensity ratio with increasing shot number suggests either a shift in the rates of formation of Si-XII and Si-III during later-stage irradiation or a shift in the relative rates of transformation of these polymorphs back into Si-I due to local heating, which occurs as the fs-laser energy dissipates into the substrate. Previous studies of the Si-XII/Si-III ratio with annealing, however, have shown that annealing should cause a decrease in the Si-XII/III ratio.[23] Therefore, it is more likely that the rate of formation of Si-XII increases relative to that of Si-III with increasing shot number, reflecting changes in the pressure profile due to the developing surface morphology and ablation processes.

The phase transformations that occur over many laser pulses would also be influenced by the formation of a-Si regions from Si-II during earlier laser pulses. An existing a-Si matrix greatly reduces the activation barrier to the nucleation of crystalline polymorphs,[25] and would therefore favor the formation of crystalline silicon polymorphs during subsequent laser pulses; such a process could produce nanocrystals of silicon polymorphs within the a-Si matrix, as observed in Fig. 2(f).

C. Relaxation with annealing and IR-absorptance

Comparing the Raman spectra of a fs-laser doped silicon annealed at various temperatures (Fig. 5(a)) with the sub-

bandgap absorptance (Fig. 5(b)) provides insights into the relationship between the silicon polymorphs and the optical properties, as well as the ability to decouple these through annealing. Undoped N_2:Si has a Raman spectra that is very similar to that of Se:Si (Fig. 1(b)), but it does not exhibit the strong absorptance into the IR region that is characteristic of the doped samples (Fig. 5(a)). This is conclusive evidence that the formation of metastable polymorphs does not play a dominant role in increasing the IR absorptance in the investigated spectral range. We note that Si-XII has a bandgap that is below the range of these absorptance spectra (230 meV or 5.4 μm).[26] In addition, Se:Si exhibits an 82% average IR absorptance after the 450 °C anneal, the point at which the high-pressure crystalline phases are undetectable by Raman spectroscopy. After the 700 °C anneal, when the a-Si has recrystallized, the average IR absorptance (44%) is still much greater than that of N_2:Si. Thus, the metastable phases in selenium fs-laser doped silicon can be annealed out while maintaining moderate IR. Such annealing treatments have been used in the past to improve the device performance of fs-laser doped silicon,[1] and the reduction of metastable silicon polymorphs during annealing might be an important contributing factor.

Changes in the Raman peak intensities can also provide insight into the transformation pathways through which the metastable polymorphs transform back to Si-I. We observe pronounced Si-XII and Si-III peaks in Fig. 5(b) after a 30 min anneal at 325 °C. Investigations of the annealing kinetics of nanoindentation-induced high pressure phases found that the Si-XII and Si-III Raman peaks were undetectable after less than 10 min of annealing at 300 °C.[35] The increased stability of the fs-laser generated silicon polymorphs could be due to their formation within the a-Si regions, as suggested from Fig. 2(f), and this has been shown to make Si-XII and S-III more thermally stable.[35] Additionally, the encapsulation of the polymorphs and a-Si within the c-Si matrix would influence the stress states, as suggested by the strain contrast visible surrounding the a-Si regions in BF-TEM images (Fig. 2(d)), and would consequently alter the kinetics of the transformation back to Si-I. The crystallization of a-Si after annealing at 700 °C agrees with previous investigations showing that the formation of c-Si from a-Si requires annealing temperatures exceeding 550 °C.[39] A more detailed study is needed in order to refine our understanding of the phase transformations that occur in fs-laser irradiated silicon with annealing.

V. CONCLUSIONS

Raman spectroscopy coupled with TEM and SEM investigations of silicon doped using fs-laser irradiation have revealed several insights into the mechanisms that lead to the formation of high-pressure phases during fs-laser irradiation. We have found that the phase of the dopant precursor does not directly impact the formation of high-pressure phases of silicon despite its influence on the microstructure, and small volumes of Si-XII and Si-III are generated under compressive stress, with more Si-XII generated than Si-III. The limited formation of a-Si, Si-XII, and Si-III and the preference for Si-XII formation over that of Si-III can be attributed to

the extremely fast pressure cycles that are generated by fs-laser irradiation. We propose that the focusing effect of the micron-scale spikes is necessary in order to achieve sufficient material ablation and pressure generation to drive high-pressure phase transformations in silicon under these irradiation conditions. This is supported by our findings that the formation of silicon polymorphs over many laser pulses is correlated with the formation of surface spikes, and that the pressure-induced phases exist only within the center of the spikes. The spatial distribution of silicon polymorphs also suggests that pressures sufficient to drive phase transformations are achieved through the collision of multiple pressure waves in the spikes, generated from the surrounding localized regions of increased ablation. By coupling Raman investigations with absorptance measurements and annealing trials, we confirm that the silicon polymorphs are not responsible for the large increase in IR-absorptance, and that the silicon polymorphs can be removed during anneals similar to those used in fs-laser optoelectronic device processing. The polymorphs are found to be more thermally stable than those generated by nanoindentation, which could be due to the stabilizing effects of the existing stress states of the polymorphs or the formation of crystalline polymorphs in an a-Si matrix. This work represents progress in understanding pressure-induced phase transformations in silicon during fs-laser irradiation and the mechanisms contributing to local pressure generation over many laser pulses. It advances our understanding of fs-laser irradiation as a processing technology for doping, has important implications in the fields of fs-laser micromachining and surface structuring, and improves the fundamental understanding of pressure-induced phase transformations in silicon.

[1]J. E. Carey, C. H. Crouch, M. Shen, and E. Mazur, Opt. Lett. **30**, 1773 (2005).

[2]M. A. Sheehy, B. R. Tull, C. M. Friend, and E. Mazur, Mater. Sci. Eng. **B137**, 289 (2007).

[3]M. A. Sheehy, L. Winston, J. E. Carey, C. M. Friend, and E. Mazur, Chem. Mater. **17**, 3582 (2005).

[4]C. H. Crouch, J. E. Carey, M. Shen, E. Mazur, and F. Y. Génin, Appl. Phys. A: Mater. Sci. Process. **79**, 1635 (2004).

[5]J. Olea, M. Toledano-Luque, D. Pastor, E. San-Andres, I. Martil, and G. Gonzalez-Diaz, J. Appl. Phys. **107**, 103524 (2010).

[6]S. K. Sundaram and E. Mazur, Nature Mater. **1**, 217 (2002).

[7]J. Bonse and J. Kruger, J. Appl. Phys. **108**, 034903 (2010).

[8]B. R. Tull, J. E. Carey, E. Mazur, J. McDonald, and S. M. Yalisove, Mater. Res. Soc. Bull. **31**, 7 (2006).

[9]B. K. Nayak, V. V. Iyengar, and M. C. Gupta, Prog. Photovoltaics 19, (2011).

[10]E. D. Diebold, N. H. Mack, S. K. Doorn, and E. Mazur, Langmuir **25**, 1790 (2009).

[11]B. R. Tull, M. T. Winkler, and E. Mazur, Appl. Phys. A: Mater. Sci. Process. **96**, 327 (2009).

[12]R. Evans, A. D. Badger, F. Falliès, M. Mahdieh, T. A. Hall, P. Audebert, J. P. Geindre, J. C. Gauthier, A. Mysyrowicz, G. Grillon, and A. Antonetti, Phys. Rev. Lett. **77**, 3359 (1996).

[13]K. T. Gahagan, D. S. Moore, D. J. Funk, R. L. Rabie, S. J. Buelow, and J. W. Nicholson, Phys. Rev. Lett. **85**, 3205 (2000).

[14]F. Costache, S. Kouteva-Arguirova, and J. Reif, Appl. Phys. A: Mater. Sci. Process **79**, 1429 (2004).

[15]M. Schade, O. Varlamova, J. Reif, H. Blumtritt, W. Erfurth, and H. Leipner, Anal. Bioanal. Chem. **396**, 1905 (2010).

[16]M. Tsujino, Rev. Laser Eng. **36**, 1218 (2008).

[17]A. Jayaraman, Rev. Mod. Phys. **55**, 65 (1983).

[18]S. R. Jian, G. J. Chen, and J. Y. Juang, Curr. Opin. Solid State Mater. Sci. **14**, 69 (2010).

[19]S. Ruffell, J. E. Bradby, and J. S. Williams, Appl. Phys. Lett. **89**, 091919 (2006).

[20]A. George, in Properties of Crystalline Silicon, edited by R. Hull (INSPEC, London, 1999).

[21]J. Crain, G. J. Ackland, J. R. Maclean, R. O. Piltz, P. D. Hatton, and G. S. Pawley, Phys. Rev. B **50**, 13043 (1994).

[22]J. I. Jang, M. J. Lance, S. Q. Wen, T. Y. Tsui, and G. M. Pharr, Acta Mater. **53**, 1759 (2005).

[23]S. Ruffell, B. Haberl, S. Koenig, J. E. Bradby, and J. S. Williams, J. Appl. Phys. **105**, 8 (2009).

[24]S. Ruffell, J. E. Bradby, J. S. Williams, and P. Munroe, J. Appl. Phys. **102**, 063521 (2007).

[25]S. Ruffell, J. E. Bradby, J. S. Williams, D. Munoz-Paniagua, S. Tadayyon, L. L. Coatsworth, and P. R. Norton, Nanotechnology **20**, 135603 (2009).

[26]B. D. Malone, J. D. Sau, and M. L. Cohen, Phys. Rev. B **78**, 161202 (2008).

[27]G. Weill, J. L. Mansot, G. Sagon, C. Carlone, and J. M. Besson, Semicond. Sci. Technol. **4**, 280 (1989).

[28]V. Domnich and Y. G. Gogotsi, Rev. Adv. Mater. Sci. **3**, 36 (2002).

[29]A. Kailer, Y. G. Gogotsi, and K. G. Nickel, J. Appl. Phys. **81**, 3057 (1997).

[30]M. J. Smith, M. T. Winkler, M. J. Sher, Y. T. Lin, E. Mazur, and S. Gradecak, "The effects of a thin film dopant precursor on the structure and properties of femtosecond-laser irradiated silicon," Appl. Phys. A: Mater. Sci. Process (submitted).

[31]K. Hayakawa, T. Fujikawa, and S. Muto, Chem. Phys. Lett. **371**, 498 (2003).

[32]Y. Yan, M. Page, T. H. Wang, M. M. Al-Jassim, H. M. Branz, and Q. Wang, Appl. Phys. Lett. **88**, 121925 (2006).

[33]Y. Izawa, Y. Izawa, Y. Setsuhara, M. Hashida, M. Fujita, R. Sasaki, H. Nagai, and M. Yoshida, Appl. Phys. Lett. **90**, 044107 (2007).

[34]D. Ge, V. Domnich, and Y. Gogotsi, J. Appl. Phys. **95**, 2725 (2004).

[35]S. Ruffell, J. E. Bradby, and J. S. Williams, Appl. Phys. Lett. **90**, 3 (2007).

[36]H. Olijnyk and A. P. Jephcoat, Phys. Status Solidi B **211**, 413 (1999).

[37]T. H. R. Crawford, G. A. Botton, and H. K. Haugen, Appl. Surf. Sci. **256**, 1749 (2010).

[38]C. H. Crouch, J. E. Carey, J. M. Warrender, M. J. Aziz, E. Mazur, and F. Y. Genin, Appl. Phys. Lett. **84**, 1850 (2004).

[39]G. L. Olson and J. A. Roth, Mater. Sci. Rep. **3**, 1 (1988).